

## **CHAPTER TWO**

### **2. LITERATURE SURVEY**

#### **2.1 Plastic Deformation**

When a metal is subjected to increasing applied loads, the strains are initially often proportional to the stress, and the material regains its original shape and/or dimensions when the load is removed. As the load is increased, a point is reached after which strains are no longer proportional to the loads and the strains are not recovered completely upon unloading. This irreversible deformation characterizes plastic deformation, and the load (or stress) at which this begins is known as the yield load (or stress). Thus, plastic deformation may be defined as deformation beyond the point of yielding, and which is not strongly time-dependent at low temperatures. In such instances, the internal structure has been irreversibly altered. The yield strength, which is a material property, is a measure of the material's resistance to flow at a given temperature and strain rate.

Metals capable of sustaining large amounts of plastic deformation before failure are said to behave in a ductile manner and those that fracture without much plastic deformation behave in a brittle manner. Ductile behaviour occurs for many metals such as low-strength steels, copper and lead. Brittle behaviour is exemplified by high strength steels, etc.

In contrast to elastic deformation which depends primarily on stress in the simplest cases, plastic deformation is typically a function of stress, temperature and the rate of straining. The microstructure of a given material is often important also. Depending on the value of the stress, temperature and strain rate, a material may exhibit various mechanisms. The mechanisms that account for the various aspects of plastic deformation are usefully treated in two categories: those that permit relative displacement of adjacent portions of the lattice over large

distances, and those that allow displacement of only one lattice spacing, or less.

Most materials are polycrystalline: they consist of many grains, each of which consists of an ordered array of atoms (on a 'lattice'). The grain boundary thickness is of atomic dimensions, hence the deformation of the grains.

The predominant mode of plastic deformation in simple crystals is crystallographic slip; twinning plays a role at low crystal symmetries, and diffusion flow is important at high temperatures and very low stresses. Slip is considered the controlling mechanism, and the deformation of polycrystals then is some average of the crystallographic slips in each grain.

The deformation in the various grains cannot be independent of each other: certain conditions must be met at the interfaces between them and this is, in fact, the major role of grain boundaries. The theory of polycrystals deformation consists essentially of treating these interactions once the properties of the grains are known. The interaction may, however, influence the deformation mechanisms inside the grains themselves and render them different from simple crystals: thus when we describe plasticity of crystals we mean that of the grains.

## **2.2 Plastic Deformation Mechanism**

Deformation that occurs beyond the point of yield, especially at low temperatures, takes place by shear or slip of one crystal plane over the other. This action is the result of the movement of microscopic defects such as dislocation through the crystal, occurring by consecutive breaking and forming of new bonds with other atoms across the slip plane. Slip takes place most readily on certain planes and in specific directions. The coordination of a particular slip plane and direction is called a slip system

and the most common slip systems are those which require the lowest stress to produce slip.

Slip occurs preferentially on the most closely packed plane and in the most closely packed directions, but if slip on these planes is constrained, other less closely packed planes become active. In the case where no such alternative modes of deformation are available, the flow stress rises above the cleavage stress and leads to brittle fracture. Apart from slip (the most common mode of plastic flow in metals) twinning is also of importance in bcc and hcp lattice structures, especially at low temperatures. In the case of fcc metals the tendency to twin increases with decreasing stacking fault energy, being greatest in silver and completely absent in aluminium<sup>2</sup>. Twinning is always preceded by some slip and is a discontinuous process whose occurrence is usually indicated by load drops on the stress-strain curve and sometimes by an audible “clicking” sound.

The motion of dislocations may be hindered or resisted by their interaction with other dislocations, impurity atoms, grain boundaries, etc. This results in the characteristic behaviour known as strain hardening, in which the material becomes stronger or harder as it deforms. If dislocations generated by a source are unable to move (glide) freely along their slip planes, a higher applied stress becomes shape change. However, it is suggested that at low plastic strain amplitudes, elastic accommodation of strain may, to some extent, compensate for the misfit arising from the non-uniform plastic deformation of adjacent grains and that all the five slip systems may not be needed.

Plastic hardening materials perform plastic deformations only upon increasing the stress level and the yield condition for plastic deformations changes during the loading process. The performance of such materials thus depends on the previous states of stress and strain. In such path-dependent cases, the elastic range of materials is, in general, expressed by means of the thermodynamic forces associated with the two internal

variables, back stress representing kinematic hardening and drag stress representing isotropic hardening

Materials often have viscous or time-dependent deformations. Time-independent plasticity is then considered as a particular limiting case of viscoplasticity. In the unified theory capable of describing cyclic loading and viscous behaviour, the time-dependent effect is unified with the plastic deformations as a viscoplastic term.

### **2.3 Creep deformation**

Creep may be defined as a deformation that occurs with time under applied constant stress (or load), which may be either static (monotonic) or cyclic. Thus, creep is a time-dependent plastic deformation phenomenon. Creep deformation under monotonic load or stress is usually performed at high temperatures (where the effect is most evident) and yields data that are often represented as a graph of strain against time (Figure 2.1). This monotonic or static creep curve shows three different stages; primary or transient stage (with decreasing creep strain-rate), secondary or steady state stage (of constant and minimum strain-rate) and tertiary or unstable stage (with accelerating strain rate).

## Creep Curves

The creep curve  $\varepsilon = f(t)$  at  $\sigma = \text{constant}$ .

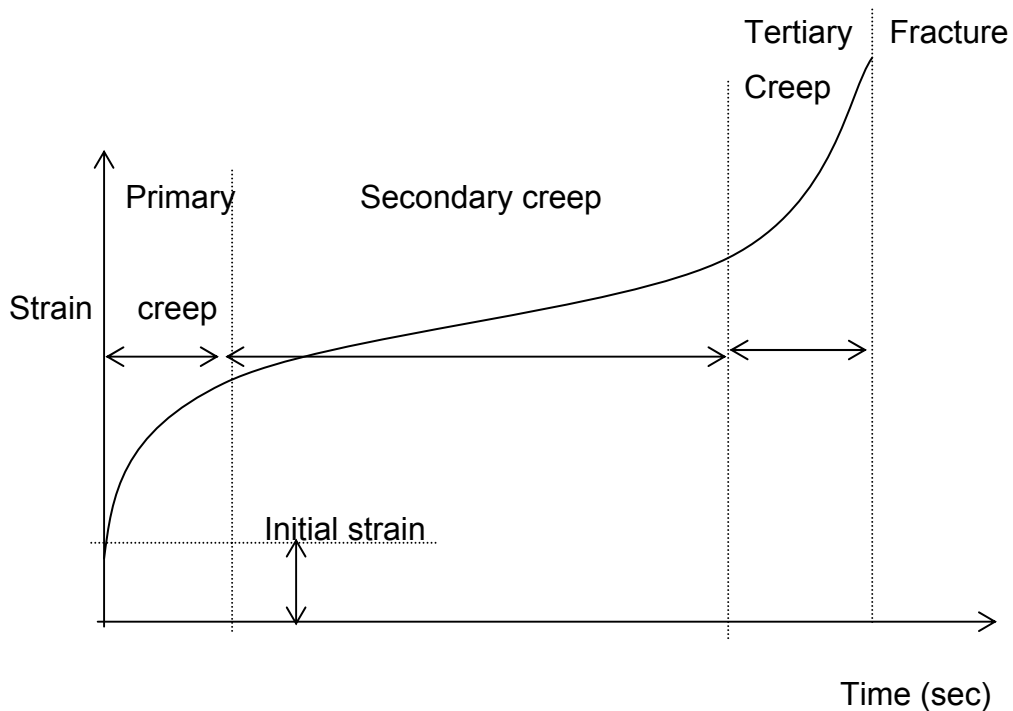


Figure 2.1 Strain versus time schematic representation of Creep Curve with basic creep regions under constant load<sup>6</sup>

- (i)  $\varepsilon = k.t^{1/3}$  (Primary creep)
- (ii)  $\dot{\varepsilon} = \frac{d\varepsilon}{dt} = \text{constant}$  (Secondary Creep)
- (iii)  $\dot{\varepsilon} = \text{increases until fracture}$  (Tertiary creep)

**Primary Creep:** Primary creep is a work hardening process during which the strain rate decreases with time.

**Secondary Creep:** Secondary creep is an equilibrium state between work hardening and softening processes or damage mechanisms. The strain rate is a constant.

**Tertiary Creep:** In the case of tertiary creep, the strain rate increases rapidly, leading to final rupture. The balance between the hardening and softening is lost, with the softening dominating.

The constant- stress creep curve exhibits the same basic shape as the constant load creep curve (Figure 2.1): an instantaneous elongation which is made up of elastic, inelastic and plastic components, followed by a period of decelerating creep, one of steady state, then accelerating creep and eventually fractures. Creep curve obtained during a constant load creep test does not yield as much information as a creep curve obtained by means of a constant- stress test. The use of a constant load implies an increasing stress as the crosssection decreases during the creep test. The creep life at constant stress is longer than that under constant load, because the material does not experience the increase of stress which occurs in a sample being tested under constant load. The occurrence of accelerated creep under constant load is due in part to the fact that the stress is increasing. The occurrence of tertiary creep under constant stress is due in part to the formation of cavities in the material which is the most common example of creep damage. The cavities act as stress concentration sites, which inevitably lead to a decrease in load carrying crosssections.

The first two stages will not leave any microstructural evidence of creep damage. Somewhere along the linear portion of (Figure 2.1), the first microstructural evidence of damage appears as individual voids or pores. The location of these first voids or holes varies, often noted at the junction of these or more grains, occasionally at nonmetallic inclusions. These individual voids grow and link to form cracks several grains long, and finally failure occurs. The ultimate rupture is by a tensile overload when effective wall thickness is too thin to contain<sup>11</sup>.

## **2.4 Creep Deformation Mechanism**

### **2.4.1 Introduction**

In general, the properties of engineering materials (mechanical strength, lattice parameter, diffusion coefficient, etc) depend on the thermo-mechanical treatment and become important for creep resistant low alloy

ferretic steels. These alloys derive most of their strength from precipitation hardening, and small changes in thermo mechanical history have large effects on the mechanical behaviour with over-ageing in service an important consideration. In practice, the steel is used in one of a few standard states and is limited in its use to temperatures below 600°C because of oxidation. Ageing in service becomes important only above 550°C. The alloy starts to transform to austenite at above 700°C and is never used structurally above 700°C, where its strength would be little better than that of pure of austenite<sup>12</sup>.

The major mechanism responsible for microstructure degradation in low alloy steels is coarsening of the carbide precipitates. The mechanism of solute hardening presents some problems. An extension of the precipitation-hardening model to individual solute atoms may, at best, apply to very dilute solutions when only interstitial solutes cause any appreciable strengthening. Randomly dispersed substitution solute atoms do not act as discrete obstacles when they are in concentrated solution, but interact with dislocations cooperatively<sup>13-17</sup>.

All real crystals contain imperfections which may be point, line, surface or volume defects, and which disturb locally the regular arrangements of the atoms. In a pure metal two types of point defect are possible, namely a vacant atomic site or vacancy, and an interstitial atom<sup>18</sup>. Impurity atoms in a crystal can be considered as extrinsic point defects. Dislocations are line defects. The behaviour and effects of these imperfections are intimately related. Dislocation lines can end at the surface of a crystal and at grain boundaries but never inside a crystal<sup>19</sup>. Thus dislocation must either form closed loops or branch into other dislocations. Crystal defects such as precipitates, voids and bubbles can occur under certain circumstances and have important effects on the properties of crystalline solids.

The mechanism of forest dislocation cutting exhibits unusual complexities. Forest dislocations can interact with glide dislocations to form attractive

junctions, where small nodal segments of dislocations can form to lower significantly the local energy of the two intersecting dislocations, making a thermally assisted intersection possible. In work hardened crystals not only are the points of intersection of forest dislocations with slip plane nearly always clustered into cell walls giving a distinctly non-random distribution, but they can also be displaced significantly under the forces exerted by an impinging glide dislocation<sup>5</sup>. Considering forest dislocations as a collection of fixed and randomly distributed point obstacles can make a satisfactory approximation and have the additional advantage of lower solubility.

When the applied stress is smaller than the mechanical threshold, dislocations must stop at various obstacles. They may be released by thermal fluctuations and then travel at a drag controlled velocity to the next obstacle. This is jerky glide. The most important mode of plastic deformation in solids is slip; at very high temperatures, it may be supplemented by diffusional mass transport and grain boundary sliding at low temperature by twinning. In slip, plastic deformation is effectively concentrated into the region between some atomic planes: in an idealised unit process, one- half of the crystal slips over the other half at an imaginary cut made between two neighbouring atomic planes. Slip occurs by the generation and propagation of dislocations. There are two types of dislocation movement, glide or conservative motion in which the dislocation moves in the surface which contains both its line and Burgers vector, and climb or non-conservative motion in which the dislocation moves out of the glide surface normal to the burgers vector. A characteristic shear stress is required for slip.

Various kinds of materials respond in different ways to an applied force. Creep occurs by grain boundary sliding, thus the more grain boundary is, the easier creep deformations will be<sup>11</sup>. The macroscopic behaviour of almost all real materials reflects the superposition of effects due to many types of obstacles and mechanisms, and occasional effects due to drag and inertia.



Creep curves are constructed from rate equations involving work hardening combining with damage accumulation equations, resulting in increasing stresses with time as the cross sectional area is lost owing to void growth. Although steady state creep is possible within the content of the scheme, it does not occur over most of the stress and temperature ranges considered.

Creep deformation is governed, basically, by thermally activated deformation processes and can occur at both low and high temperatures, although most investigations of the phenomenon have been at high temperatures. Most of the available data concerning deformation during creep testing are presented in the form of steady state creep rates. Information from such data has led to the identification of regions of stress-temperature space in which different and often competing physical mechanisms control the strain rate, and are often presented in the form of deformation-mechanism maps (see section 2.5).

The physical mechanisms that cause creep deformation differ markedly for different classes of materials. Even for a given material, different mechanisms act in various combinations of stress and temperature. These physical mechanisms are related to microscopic processes such as the motions of atoms, vacancies, dislocations, or molecules, which occur in a time-dependent manner and more rapidly at higher temperatures.

In polycrystalline solids the number of mechanisms in creep deformation often compete with one another. Among these, the principal mechanisms for fracture are void growth and coalescence and, in the case of high strength alloys, microstructure degradation such as precipitates coarsening. The three major deformation mechanisms include<sup>20</sup> plasticity controlled by glide of dislocations through an obstacle field, power-law creep controlled by climb dislocations over obstacles, and diffusional creep under the influence of a stress-induced chemical potential difference. The latter two mechanisms occur at high temperatures:-

diffusional flow at high temperatures and high stress, and dislocation climb at higher temperature and lower stresses.

For some metals at relatively high stresses and low temperatures, the rate controlling mechanism is often regarded as dislocation glide through an obstacle field that may be provided by forest dislocations or precipitate. At higher temperatures and lower stresses, the rate controlling process becomes dislocation climb rather than glide. At intermediate stress and temperature, conditions between the glide (plasticity) and climb (power law creep) exist. This intermediate behaviour is known as power law breakdown. Power law breakdown is usually described by empirical equations or may be described by a combination of glide and power law equations.

Dislocation glide is by far the most common in plasticity with other forms assisting or facilitating the process. Generally, the stress contributing to the flow is divided into two components: namely, athermal or internal stress component, and a thermal or effective stress component<sup>21</sup>. The athermal stress describes the long range kinetic hardening associated athermal obstacles, while the thermal (effective) stress describes the net stress available to drive dislocation past thermally penetrable obstacles. In the limit when the thermal stress component is zero, slip is athermal in the sense that obstacles to dislocation motion can be overcome only by increasing the stress or by reducing the obstacles strength through recovery or re-arrangement. Thus for athermal slip the rate of deformation depends not only on stress, temperature and microstructure, but also on the rate of increase of the applied stress.

Each mechanism of deformation can be described by flow kinetics and evolution kinetics<sup>6</sup>. The flow stress is ascribed to be a function of the temperature, deformation rate and a parameter that characterizes the mechanical structure of the material. The structure parameter corresponds to a certain configuration of dislocation structure and determines the mechanical state of the materials. It differs from the

microstructure, which describes the metallurgical state of materials. The whole history of the material, for instance heat treatment and pre-deformation, can therefore be represented by the structure parameter<sup>22</sup>. Equations describing these flow mechanisms have similar forms and express the strain rate in terms of the frequency factor, the stress raised to some power and an Arrhenius term.

## 2.4.2 Kinetics and Rate Equations

### 2.4.2.1 Constitutive Laws

As has been stated above, there are two different types of kinetics that are conveniently separated in plasticity: flow kinetics, which describe dislocation glide at a given structure or state of the material; and evolution kinetics, which describe the influence of strain-rate and temperature on the rate of change of structure (state)<sup>6</sup>.

#### *Flow Kinetics*

Each mechanism of deformation can be described by a flow kinetics equation that relates strain rate to the stress, temperature and to the structure of the material at that instant<sup>1,2</sup>.

$$\dot{\epsilon} = f(\sigma, T, S_i, P_j) \quad 2.1$$

The set of  $i$  quantities  $s_i$  are the state variables which describe the current microstructural state of the materials. The sets of  $j$  quantities  $p_j$  are the material properties: lattice parameter, atomic volume, bond energies, moduli, diffusion constants, etc;. These can be regarded as constant except when the plastic properties of the different materials are to be compared.

## Evolution Equation

The state variables  $s_j$  change generally as the deformation progresses. Evolution kinetic equations describe their rate of change, one for each state variable<sup>1,2</sup>:

$$\frac{ds_i}{dt} = g(\sigma_i, T, S_i, P_j) \quad 2.2$$

Where  $t$  is the time, the coupled set of equation (2.1) and (2.2) is the constitutive law for a mechanism. Both approach reduce the constitutive law to a single equation if constant structure ( $s_i = s_{ij}$ ) and steady state ( $\frac{ds}{dt} = 0$ ) conditions are assumed<sup>1</sup>:

$$\dot{\epsilon} = f(\sigma_i, T) \quad 2.3$$

This implies that the internal variables such as dislocation density and arrangement, grain size, etc no longer appear explicitly in the rate equations because they are determined by the external variables of stress and temperature. The properties  $p_j$  are constant for a given material.

At low temperatures a steady state is rarely achieved. For the dislocation-glide mechanisms, a constant structure formulation is used. The equations describe flow at a given structure and state of work hardening.

At high temperatures, deformation materials quickly approach a steady state, and the equations are appropriate for this steady state behaviour.

### 2.4.2.2 Rate Equations

Plastic deformation is temperature dependent and because the waiting time depends on the occurrence of a large enough amplitude, it is also

time and rate dependent. This is the physical cause of rate and temperature dependence. The amplitude of fluctuation is a probabilistic event and is defined by statistical thermodynamics. The average is a probabilistic event and is defined by statistical thermodynamics. The average frequency of the random occurrence of large enough amplitude is expressed by the elementary rate  $k$  for all thermally activated processes as<sup>6</sup>.

$$k = \nu \exp\left[-\frac{\Delta G(W)}{kT}\right] \quad 2.4$$

where  $\Delta G(W)$  is the apparent activation energy, the energy supplied by the heat content of the solid, which is a rigorously defined function of the work  $W$ . The effect of these two sources of energy is the breaking of the bond.

### 2.4.3 Thermally activated glide

At relatively low temperatures and high stresses, the rate controlling mechanism is dislocation glide through an obstacle field provided by a forest dislocation or precipitate. Equations for thermally activated glide often express the steady state shear rate  $\dot{\gamma}$  as a function of the applied shear stress  $\tau$  normalized with reference to the temperature compensated shear modulus  $\mu$ , the activation energy  $\Delta G$  and the absolute temperature  $T$  in the form generally described by an Arrhenius equation<sup>7</sup>. The equation for thermally activated glide is written as<sup>2, 23</sup>:

$$\dot{\gamma} = \nu \left(\frac{\tau}{\mu}\right)^2 \exp\left(\frac{-\Delta G}{kT}\right) \quad 2.5$$

where the frequency factor  $\nu$  is usually assigned a value of the order  $10^{11} \text{ s}^{-1}$ ,  $k$  is the Boltzmann's constant and  $\mu$  is the temperature compensated shear modulus. In this case the probability term is a function of the applied stress and  $\Delta G$  is written as<sup>2</sup>:

$$\Delta G = \Delta F \left\{ 1 - \left( \frac{\tau}{\tau_0} \right)^p \right\}^q \quad 2.6$$

Where  $\tau$  is a material constant, being the shear strength in the absence of thermal energy,  $\Delta F$  is the total free energy (activation energy) required to overcome obstacles without the aid of the external stress. It is believed to depend on the strength of obstacles to flow. For precipitate hardened alloys where the precipitates are strong obstacles to flow, the activation energy is assumed to be  $\Delta F \cong 2\mu b^3$ , and for weak obstacles  $\Delta F$  can be as low as  $0.05 \mu b^3$ ,  $\tau_0$  is a stress term representing average obstacle strength, with  $T$  and  $k$  being respectively the absolute temperature and Boltzmann's constant. The constants  $p$  and  $q$  are taken to represent the average shapes of the flow obstacles,  $p$  describing the shape of tail and  $q$  the shape of the peak. Values of unity for each of these represents an array of cylindrical shaped barriers. If  $\Delta F$  and  $\tau_0$  are functions of the degree of work hardening, i.e., functions of the structure of the material, then equation (2.6) would be capable of describing non-steady deformation behaviour under constant-applied stress conditions, since these quantities may be expected to increase with increasing strain, giving rise to a falling strain rate.

With the aid of equations (2.5) and (2.6), the rate equation for discrete obstacle controlled plasticity can be written as:

$$\dot{\gamma} = v_0 \exp \left[ - \frac{\Delta F}{kT} \left( 1 - \frac{\sigma_s}{\tau_0} \right) \right] \quad 2.7$$

Table 2.1: Characterization of obstacle strength<sup>2</sup>

Obstacle Strength	$\Delta F$	$\frac{t}{L}$	Examples
Strong	$2\mu b^3$	$>\mu b/L$	Dispersions; large or strong precipitate (spacing, L)
Medium	0.2- $1.0\mu b^3$	$\approx\mu b/L$	Forest dislocation; radiation damage, small or weak precipitate spacing, L
Weak	$<0.2\mu b^3$	$\ll\mu b/L$	Lattice resistance; solution hardening (solute spacing, L)

Solute atoms (alloys or impurities) introduce a friction like resistance to slip, caused by interaction of the moving dislocations with stationary weak obstacles, e.g. single solute atoms in a very dilute solutions, or local concentration fluctuations in more concentrated solutions.

A dispersion of strong and stable particles of a second phase, such as the particles in SAP (aluminium containing  $Al_2O_3$ ), T-D Nickel (Nickel containing  $ThO_2$ ) or low-alloy steels (steels containing dispersions of carbides) cause a gliding dislocation to move only by bowing between and bypassing them. This gives a contribution to the flow strength, which scales as the reciprocal of the particle spacing and which has high activation energy (Table 2.1). The activation energy as used in equation (2.7) is so large that it leads to a flow stress which is almost athermal, but for sufficiently worked alloys the yield stress will regain the temperature dependence which characterizes forest hardening. However, where thermally activated cross-slip at particles occurs<sup>24,25</sup>, work hardening becomes relaxed, leading to a lower flow strength<sup>2</sup>.

Precipitates may resist dislocation motion according to their fineness. In

finely dispersed form, the moving dislocations can cut precipitates. If the density of the particles is high, then the flow strength is high (high  $\tau$ ) but strongly temperature-dependent (low  $\Delta F$ ). Increasing coarseness of precipitate increasingly causes it to behave like a dispersion of strong particles.

*Lattice resistance limitation of plasticity (Peierls force)*

In addition to discrete obstacles, the atomic structure itself may limit the velocity of a dislocation in most polycrystal solids. As the dislocation moves, its energy fluctuates with position, the amplitude and wavelength of fluctuations being determined by the strength and separation of the inter-atomic or inter-molecular bonds. Under the applied stress and thermal energy (temperature) the dislocation advances against lattice barriers by throwing forward kink pairs which subsequently spread apart<sup>26,27</sup>. The limit to this dislocation velocity is due to the nucleation rate of kink pairs. The Gibbs free energy of dislocation for this event is<sup>2</sup>:

$$\Delta G(\sigma_s) = \Delta F_p \left[ 1 - \left( \frac{\sigma_s}{\tau_p} \right)^p \right]^q \quad 2.8$$

where  $\Delta F$  is the Helmholtz free energy of an isolated kink pair; and  $\tau$  is the flow stress at Zero Kelvin (OK). The rate-equation for plasticity limited by a lattice resistance is given as<sup>2</sup>:

$$\dot{\gamma} = \dot{\gamma}_p \left( \frac{\sigma_s}{\tau} \right)^2 \exp \left\{ - \left( \frac{\Delta F_p}{kT} \right) \left( 1 - \frac{\sigma_s}{\tau_p} \right)^p \right\}^q \quad 2.9$$

The values of  $p$  and  $q$  can be determined from experimental data. Since  $\Delta F$  is usually small, the pre-exponential stress is retained (not ignored as



in the case of discrete obstacles). The stress due to lattice resistance is known as the Peierls' stress.

### *Plastic flow by mechanical twinning*

Twinning is a variety of dislocation glide which involves the motion of partial, rather than complete dislocations. It occurs at very low temperatures. It is an important deformation mechanism in hexagonal closed-packed and body-centred cubic metals. It is less important in face-centred cubic metals but the tendency increases with decreasing stacking fault energy. The strain-rate equation for twinning is of the form:-

$$\dot{\gamma} = \dot{\gamma}_p \exp \left[ \left( -\frac{\Delta F_n}{kT} \right) \left( 1 - \frac{\sigma_s}{\tau_t} \right) \right] \quad 2.10$$

where  $\Delta F_N$  is a temperature-dependence activation free energy of nucleation of a twin without the aid of external stress,  $\dot{\gamma}_p$  is a constant with dimensions of strain-rate and includes the density of available nucleation sites and the strain produced by successful nucleation; and  $\tau_t = \tau(t)$  is the stress required to nucleate twinning in the absence of thermal energy.

### *Non-steady state behaviour*

In the above discussion on rate equations either steady-state or constant structure have been assumed, in which case the rate equation may be expressed in the form of equation (2.3). For non-steady state of flow, however, the state variables,  $S_i$  (i.e., dislocation density, etc) change with time or strain rate. That is,  $S_i(t \text{ or } \gamma)$ . Thus, using  $S_i(t)$ , we have  $\dot{\gamma} = f(\sigma, T, t)$ , so that by integration it gives the strain for the loading history as:

$$\gamma = [\sigma_s, T, t] \quad 2.11$$

In general, the total strain is the sum of the elastic ( $\gamma_e$ ) and plastic ( $\gamma_p$ ) components, that is

$$\gamma_e = \frac{\sigma_s}{\mu} \quad \text{and} \quad \gamma = \frac{\sigma_s}{\mu} + \gamma_p \quad 2.12$$

Thus, in the case where non-steady state or transient flow occurs, the total strain for the loading history, rather than the strain rate, is of paramount importance.

At ambient temperatures, metals work-harden, and the flow stress, at a given strain rate, changes with time. In general, a work-hardening law can describe stress-strain curves, empirically, and for tensile straining, this is given as:

$$\sigma = \sigma_0 + k\varepsilon_{pt}^m \quad 2.13$$

where  $\varepsilon_{pt}$  is the plastic tensile strain, and  $m$  is the strain-hardening exponent. Thus, in making the plastic strain the subject of equation (2.13) we obtain:

$$\gamma_{pt} = \left\{ \left( \frac{\sigma_s - \sigma_{os}}{k} \right) \right\}^{1/m} \quad 2.14$$

In terms of equivalent shear stress and strains we have<sup>2</sup> :

$$\gamma_{pt} = \left\{ \left( \frac{\sigma_s - \sigma_{os}}{k_s} \right) \right\}^{1/m} \quad 2.15$$

where  $k_s = \frac{k}{3^{m+1/2}}$ , and  $\sigma_{os}$  is the initial shear strength.

The integrated form of the plastic strain is not a well-defined deformation

variable because it does not reflect in a unique way the current microstructure of the deformed material and, more particularly, the density and arrangement of dislocations and or cell structures. Thus, for a rate equation to completely describe the history of the material during the transient behaviour, the evolution of its structure must be taken into account.

Hart<sup>28</sup> suggested that, instead of the plastic strain, an evolutionary variable  $c$ , called the "hardness state" has to be employed to describe the memory of a material for its past history. Kocks<sup>29</sup> also suggested that there exist a somewhat different (single) state parameter, known as "mechanical threshold" that can also describe work hardening in a satisfactory way. However, it is pointed out that a single state variable is not adequate<sup>30</sup> to describe phenomena in which the load is cyclic or during the few percent or tenths of a percent of strain when the strain is imposed or changed abruptly during monotonic loading. In general it is regarded that the kinetic equation may be governed by more than one structural parameter ( $S_i, i = 1,2,3...$ ) such as dislocation density, cell size, etc, that evolve with different rates. Each of these structural parameters is expected to assume its own stationary value after a certain transient strain.

#### 2.4.4 Power law creep

At higher temperatures and lower stresses, the rate controlling process becomes dislocation climb rather than glide.

Steady state deformation in power law is generally expressed in terms of the Dorn equation which may be written as:<sup>2,3</sup>

$$\dot{\epsilon} = A \frac{D_{\text{eff}} \mu b}{kT} \left( \frac{\tau}{\mu} \right)^n \quad 2.16$$

and

$$D_{\text{eff}} = D_0 \exp\left(-\frac{Q_v}{RT}\right)$$

Where  $A$  and  $n$  are constants,  $b$  is the Burgers vector, and  $D_{eff}$  is an effective diffusion coefficient reflecting contributions from vacancy diffusion in the lattice  $D_v$ , and dislocation core diffusion  $D_c$ . Higher values for  $n$ , particularly at lower temperatures, may be rationalized to some extent by including dislocation core diffusion effects which become dominant at lower temperatures and higher stresses, which may be written as<sup>2</sup>.

$$D_{eff} = D_v + 10 \frac{a_c D_c}{b^2} \left( \frac{\tau}{\mu} \right)^2 \quad 2.17$$

Assume that the apparent activation energy depends on applied stress in the power law creep regime suggests that the activation energy term appearing in equation (2.17) could be replaced by an activation energy of the form used in the glide equation (2.2). That is, the probability that a climb event occurs depends, as with glide, on the applied stress and a flow stress. If the flow stress term increases with increasing deformation, i.e., with increasing degree of work hardening, then the Dorn equation with a modified exponential term is capable of describing primary creep. In the present description of deformation, the Dorn equation is used to describe deformation limited by climb, with the theoretical value of  $A$  and  $n$  together with a modified exponential term as<sup>23</sup>.

$$\dot{\epsilon} = D \frac{\mu b}{kT} \left( \frac{\tau}{\mu} \right)^3 \quad 2.18$$

Where  $D_{eff}$  is written in terms of equation (2.16) and each of the diffusion coefficients in equation (2.16) are written as

$$D = D_{0exp} \left\{ \frac{-Q}{RT} \left( 1 - \frac{\tau}{\mu} \right)^p \right\}^q \quad 2.19$$

The empirical content of equation (2.19) does not appear in the constants  $A$  and  $n$ , which have no physical significance if their values are different from 1 and 3 respectively. They are contained in the values of  $p$  and  $q$  which may be physically interpreted, in principle at least, in terms of the shape and distribution of energy barriers opposing climb, and the flow stress  $\sigma$ , represents the degree of work hardening.

#### 2.4.5 Power Law Breakdown

At stresses above  $10^{-3}\mu$ , the simple power-law breakdown and strain rates are greater than predicted by the power-law equation, the process is evidently a transition from climb control to glide flow.

Many attempts have been made to describe this transition empirically. The proposed rate equation for both power-law creep and power-law breakdown is<sup>2</sup>:

$$\dot{\epsilon} = A'_2 \frac{D_{eff} \mu b}{kT} \left[ \sinh \left( \alpha' \frac{\sigma_s}{\mu} \right) \right]^{n'} \dots\dots\dots 2.20$$

This reduces to the power law creep equation at stresses below  $\sigma_s = \mu / \alpha'$

#### 2.4.6 Diffusional creep

Diffusional creep which tends to be the dominant deformation mechanism at low stresses and higher temperatures may occur by either bulk or grain boundary diffusion. Diffusional creep has been included in the calculation scheme and is represented by the equation<sup>3</sup>.

$$\dot{\epsilon} = \frac{42\tau\Omega D_{eff}}{kTd^2} \quad 2.21$$

and 
$$D_{eff} = D_v + \frac{p_i \delta_b D_b}{d} \quad 2.21a$$

where  $d$  is the grain size,  $D_b$  is the boundary diffusion coefficient and  $\delta_b$  the effective thickness of the boundary. At high temperatures, lattice diffusion controls the rate; the resulting flow is known as Nabarro-Herring creep and its rate scales as  $D_v/d^2$ . At lower temperatures, grain boundary diffusion takes over; the flow is then called Coble creep, and scales down  $D_b/d^3$ .

#### 2.4.7 Damage accumulation

During uniaxial creep deformation, damage is due to the presence of grain boundary voids. It is believed that voids are nucleated at an early stage in the creep life and that void growth is the major controlling factor in the damage accumulation. As with deformation mechanisms, a number of factors may control void growth. Three major mechanisms considered are growth due to diffusion of material from void along grain boundaries, growth due to diffusion of the material along the surface of the growing void, and void growth as a result of power law creep. The rate of damage accumulation can be written (in terms of equivalent shear stress rather than the normal stress) as<sup>2</sup>:

$$\frac{df}{dt} = \frac{23^{1/2} \delta_b d_b \Omega \mu}{k T l_v^3 f_v^{1/2} \ln(1/\sqrt{f_v})} \left\{ \frac{\tau}{\mu} \right\} \quad 2.22$$

where  $\delta_b$  is the grain boundary thickness,  $D_b$  is the grain boundary diffusion coefficient,  $\Omega$  is the atomic volume and  $l_v$  is the void spacing. The major problem in using this equation is the choice of a suitable value for the void spacing. Evidence seems to suggest that the void spacing is inversely proportional to the applied stress, and has been written as:

$$l = kd \left( \frac{\tau}{\mu} \right)^{-1} \quad 2.23$$

## 2.4.8 Softening Kinetics

### *Recovery*

The basis of all recovery – creep theories is the knowledge that materials harden with strain and soften with time while being heated. When these two processes occur simultaneously as in high temperature creep, deformation is bound to take place. These ideas were first formulated by Bailey<sup>31</sup> and Orowan<sup>32</sup>, and were subsequently elaborated by Cottrell and Aytakin<sup>33</sup>, Mott<sup>34</sup>, Mclean and Hale<sup>35</sup>, Mclean<sup>36</sup>, Lagneborg<sup>37</sup> and Gittus<sup>38</sup>. According to this theory, a balance between strain hardening and recovery will exist in the secondary creep stage, producing a steady state creep rate.

Although the consideration of the concurrent strain hardening and recovery processes certainly has a true physical background, the recovery theory could be considered as phenomenological in the sense that it frequently does not take into account the detailed mechanism by which the glide process or the recovery operates. The formulation of the recovery creep model is such that in principle it could encompass any thermally activated glide process. Accordingly in this respect, the recovery creep theory model as such is incommensurable with the climb theory and the dislocation –jog theory. In practice the dislocation climb theory as expressed by Weertman<sup>39</sup> inherently involves a balance between strain hardening and recovery, and may be considered as a recovery –creep model .

Although the earlier recovery-creep models did not describe the details of the deformation process, the most recent formulations by Mclean and Lagneborg consider the mechanisms in some detail. In agreement with direct observation these authors assume the dislocations to be arranged in a three dimensional network. The creep process consists of consecutive events of recovery and strain hardening. The strength is

provided by the attractive and repulsive junctions of the network. Some of these junctions will break as a result of thermal fluctuations; those connected with the longest dislocation break most frequently. The released dislocations move a certain distance until they are held up by the network, and thereby give rise to a strain increment and also to an increase in the internal stress, i.e., strain hardening, since the expanding dislocation increases its length and therefore dislocation density. Simultaneously, recovery of the dislocation network takes place. It is assumed that this occurs by a gradual growth of the larger meshes shrinkage of the smaller meshes, in analogy to grain growth.

Upon the application of load, the material will strain harden according to the equation<sup>40</sup>.

$$\sigma = \sigma_0 + \alpha Gb\sqrt{\rho} \quad 2.24$$

The steady state creep rate,  $\dot{\epsilon}_s$ , for recovery creep deformation in dislocation creep regime at elevated temperature of pure metals and alloys is commonly described by the Bailey–Orowan equation<sup>31-32</sup>.

$$\dot{\epsilon}_s = r/H \quad 2.25$$

Where  $H$  is strain hardening rate give by<sup>34-35</sup>:

$$H = \left( \frac{d\sigma}{d\epsilon} \right)_r \quad 2.26a$$

And at high temperature ( $T > 0.5T_m$ ) the material will also recover (decrease its dislocation density). The recovery rate ( $r$ ) is defined by<sup>31-32</sup>.

$$-r = \left( \frac{d\sigma}{dt} \right)_\epsilon \quad 2.26b$$



Recovery takes place because, at these temperatures, the self diffusion is fast and it is possible for the dislocations to climb and annihilate. Equation (2.26) is the fundamental equation for the traditional theory for recovery. As pointed out by Orowan<sup>32</sup>, an assumption is made in the theory that  $r$  depends only on the temperature and the stress. If this assumption is made, equation (2.26) demands, at constant temperature and stress, a constant rate of creep, and this cannot be reconciled with deceleration and extremely high rate of flow at the beginning of creep. In order to overcome these difficulties, it can be assumed that  $r$  depends also on the entire stress-strain history of the specimen. Equation (2.26) can be properly applied only to the steady state deformation stage in which strain rate is a constant. It can not be applied directly to transient creep in which creep rate is a function of time.

The slowest step in this process will control the recovery speed and in this case it is the self diffusion.

$$r = r_0 e^{-Q / RT} \quad 2.27$$

$$d\sigma = Hd\varepsilon - rdt = 0 \quad 2.28$$

At steady state creep i.e.,  $\sigma = \text{constant}$  i.e. we have a balance between the production and annihilation of dislocations. The steady state creep rate in recovery creep can approximately be described by Norton's Law<sup>41</sup>:

$$\dot{\varepsilon} = k_s \left( \frac{\sigma}{G} \right)^n \frac{G.b}{RT} e^{-Q / RT} \quad 2.29$$

where  $n$  lies between 4 and 6.

For the evolution kinetics in low alloy steels where complex structures of carbide precipitate and dislocation tangles as a result of quenching process, softening could be attributed to both carbide growth and tangled dislocations re-arrangement and annihilation.

The concept of hardening is thought to be controlled by the competition of storage and annihilation (rearrangement) of dislocations, which processes are assumed to superimpose in an additive manner<sup>13-16</sup>.

During recovery, the mean radii of precipitates increase with time and there is a general re-arrangement of the material internally. In the case of precipitate coarsening, the precipitate growth rate can be expressed as<sup>20</sup>.

$$\frac{dr}{dt} = \frac{A'}{RT} \exp\left(-\frac{Q}{RT}\right) \quad 2.30$$

The structure parameter term can be introduced by writing it in terms of the precipitate spacing as

$$\lambda = \frac{\alpha b \sqrt{v_f}}{r} \quad 2.31$$

where  $v_f$  is the volume fraction of the precipitate,  $r$  is the radius of the grain and  $A'$  is a factor which depends on the surface energy, solubility of precipitate in the matrix, etc., substituting equation (2.30) into equation (2.31) yields:

$$\frac{d\lambda}{dt} = \frac{A'' \lambda^3}{RT} \quad 2.32$$

where  $A'' = A \exp\left(-\frac{Q}{RT}\right) \quad 2.33$

integrating equation (2.23) results in

$$\lambda = \left[ \frac{At}{RT} \exp\left(-\frac{Q}{RT}\right) + \frac{1}{\lambda_0^3} \right]^{-1/3} \quad 2.34$$

The factor  $A$  contains terms that are temperature dependent, such as volume fraction of the precipitate and the solute concentration of the matrix. The evolution for  $\dot{\epsilon}$  can be derived by specifying the evolution of the dislocation density.

## 2.5 Deformation Mechanism Maps

All maps are divided into fields and the competition between mechanisms is conveniently summarized in the diagrams. They show the range of stress and temperature or sometimes strain-rate and stress in which we expect to find each sort of creep. They also show where plastic yielding occurs, and where deformation is simply elastic. The field boundaries are the loci of points at which two mechanism contribute equally to the overall strain- rate, and are computed by equating pairs of rate equations and solving for stress as a function of the temperature .

In situations in which two or more processes are involved in causing deformation, the processes may be independent or sequential<sup>42</sup> . For sequential processes, the creep rate is governed by the rate of the slowest necessary step. However, when two or more processes occur independently, the overall creep rate is the sum of all the rates of the independent processes taking place, so that the measured rate is determined primarily by the fastest process. Power law creep and diffusional flow are independent flow mechanisms involving different defects<sup>2</sup> .To a first approximation, their strain rates add. Power law creep and glide do not. Both processes involve the same defect; they describe the same dislocations moving under different conditions. As the gliding part of the dislocation motion become more important with increasing stress, the climbing part becomes less important. At the boundary, power law creep is not necessary at all. Here power law creep and glide plasticity are treated as alternative mechanisms.

Furthermore, since dislocation and diffusional processes are independent, one of these processes can be defined as being dominant when the

contribution to the overall creep rate made by the other independent processes is so small that it can be ignored.

This concept of a dominant creep process can be extended to provide an indication of the conditions under which, say, dislocation or diffusional creep processes would be expected to govern creep behaviour at temperatures of about  $0.4T_m$  and above. The exact locations of the boundaries between adjacent creep regimes obviously differ for different materials. Moreover, even for the same material, the stress/temperature ranges over which a particular mechanism is dominant can be dependent on such micro structural variables as grain diameter. The accuracy of the maps reflects that of the experiments.

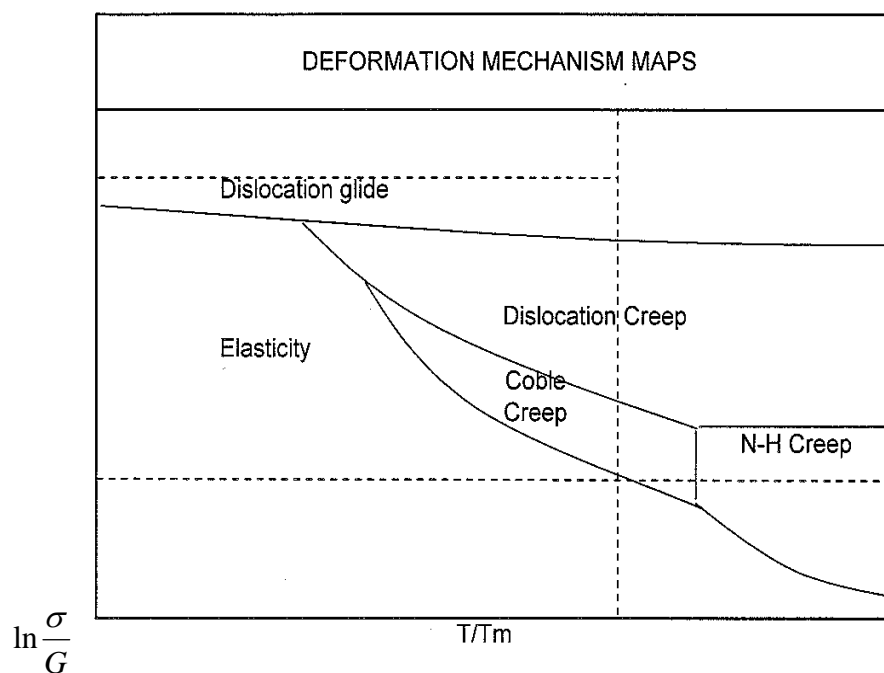


Figure 2.2 Deformation Mechanism Maps at different stresses and temperatures<sup>2</sup>

## 2.6 Other Existing Empirical Methods of Calculating Creep Parameters

### 2.1 Introduction

Rather than considering steady state deformation in isolation, there has been a renewed trend towards modelling of creep curves as a whole by considering them in terms of concurrent work hardening and damage accumulation effects. Such treatments may be empirical in form such as in the continuum damage mechanics approach<sup>42</sup> and the  $\theta$ -projection concept<sup>7</sup> or may use semi-empirical equations similar to those shown above to describe deformation together with the relevant equations to describe creep. In such cases, steady state creep is not explicitly described as such but approximately steady state behaviour over a time range may occur when work hardening and damage accumulation terms sum suitably. Four techniques are outlined below giving their merits and demerits with respect to the present study. The application of each approach in determining creep of low alloy steel similar to one used in this study is explored.

#### 2.6.2 Estrin –Mecking Method

##### *One parameter approach*

In one parameter model, the glide kinetics that are generally described by the Arrhenius equation is considered in the form of a power law as is usual in phenomenological modeling. For a prescribed strain rate we have

10

$$\sigma = \sigma_0 \left( \frac{\dot{\epsilon}}{\dot{\epsilon}_0} \right)^{1/m} \quad 2.35$$

For a prescribed stress we have

$$\dot{\epsilon} = \dot{\epsilon}_0 \left( \frac{\sigma}{\sigma_0} \right)^m \quad 2.36$$

Where  $\dot{\epsilon}_0$  is a referential plastic strain rate,  $1/m$  is the strain rate hardening exponent. The hardness (athermal stress)  $\sigma_s$  due to short-range dislocation interaction is expressed by the standard relation,<sup>(10,43)</sup>

$$\sigma_s = \alpha G b \rho^{1/2} \quad 2.37$$

here  $G$  is the shear modulus,  $b$  is the magnitude of the burgers vector of the dislocations and  $\alpha$  is a numerical constant. The evolution of  $\sigma_s$  can be derived by specifying the evolution of the dislocation density  $\rho$ . Here the concept of hardening is deemed to be controlled by the competing of storage and annihilation of dislocations. The equation for the evolution reads:<sup>(10,14,43)</sup>

$$\frac{d\sigma_s}{d\varepsilon} = k_1 \rho^{1/2} - k_2 \rho \quad 2.38$$

In analyzing the Kocks-Mecking single parameter approach by Estrin and Mecking<sup>10</sup>, combining equation (2.37) and (2.38), one readily obtains the evolution equation for the structure, or hardness parameter  $\sigma_s$ . This can be expressed in terms of an evolution equation describing the change in work hardening as rate with strain as:<sup>10</sup>

$$\frac{d\sigma_s}{d\varepsilon} = \theta_0 \left( 1 - \frac{\sigma_s}{\sigma_0} \right) \quad 2.39$$

with

$$\theta_0 = \frac{\alpha G b k_1}{2} \quad 2.40a$$

and  $\sigma_s = \alpha G b (k_1 / k_2)$  2.40b

From equation (2.39) the hardness parameter  $\sigma_s$  evolves in the course of plastic deformation towards a steady state value  $\sigma_s$  i.e., towards a state

where the hardness parameter does not vary with the strain,  $\frac{d\sigma}{d\varepsilon} = 0$ .  $\sigma_s$  represents the maximum or saturation stress which can be attained.  $\theta_0$  is the initial work hardening rate.

Equation (2.40) can be integrated to give the flow stress in terms of the strain rate as:

$$\sigma = \sigma_0 \left[ 1 - \left( 1 - \frac{\sigma_y}{\sigma_0} \right) \exp \left( - \frac{\varepsilon \theta_0}{\sigma_0} \right) \right] \quad 2.41$$

Where  $\sigma_y$  is the yield stress term representing the initial state of hardening of the material, it is recognized that  $\theta_0$  is independent of the strain rate and depends on the temperature through the temperature dependence of  $G$  only. The temperature and strain rate dependence of  $k_2$  on the other hand, give rise to the corresponding dependence of  $\sigma_s$ , which is assumed to have a power law form suggested by experimental evidence<sup>10, 43-46</sup>.

$$\frac{\sigma_s}{\sigma_{s0}} = \left( \frac{\dot{\varepsilon}}{\dot{\varepsilon}_0} \right)^{1/n} \quad 2.42$$

This form is equivalent to assuming  $k_2 \approx (\dot{\varepsilon} \dot{\varepsilon}_0)^{-1/n}$ . In equation (2.42), the normalization constant  $\sigma_{s0}$  is the saturation value of the hardness parameter associated with a reference strain rate  $\dot{\varepsilon}_0$  that can be arbitrarily chosen. Equation (2.41) is of empirical nature. Its relationship to the dependence between the strain rate, stress, and temperature for steady state creep suggests that it actually covers both high temperature and low temperature ranges. At low temperatures,  $n$  is dependent on temperature, assuming the cross slip theory<sup>44</sup> with  $\sigma_{s0}$  and  $\dot{\varepsilon}_0$  is constant. In the high temperature range,  $n$  is constant and is approximately equal to 4, while  $\dot{\varepsilon}_0$  attains the Arrhenius type temperature dependence

$\left(\exp\left(-\frac{Q}{kT}\right)\right)$  with  $Q$  being the activation energy for self diffusion. For constant temperature  $\dot{\epsilon}$  at high temperature is constant. The recovery term above implies that static recovery of the Bailey –Orowan type can be neglected.

For dynamic loading the hardening coefficient defined as slope for Kock-Mecking<sup>16</sup> and Estrin-Mecking<sup>10</sup> are given by equation (2.43) and (2.44) respectively below.

$$\theta = \theta_0 \left(\frac{\dot{\epsilon}}{\dot{\epsilon}_0}\right)^{1/m} \left[1 - \frac{\sigma}{\sigma_s}\right] \quad 2.43$$

$$\theta\sigma = \frac{1}{2} (k\alpha^2 b^2) G^2 \left(\frac{\dot{\epsilon}}{\dot{\epsilon}_0}\right)^{2/m} \left[1 - \left(\frac{\sigma}{\sigma_s^*}\right)^2\right] \quad 2.44$$

The evolution in the form of equation (2.38) was designed to describe materials where dislocation storage is controlled by the total dislocation density. As mentioned above, the example in question was a coarse grained (mono-crystalline) single-phase material. The dislocation mean free path in such a material is given by the average dislocation spacing  $\rho^{1/2}$ , in a random dislocation arrangement or by the cell or sub-grain size in an ‘organised’ dislocation structure. For a material containing non shearable second - phase particles or a material with a small grain size, the mean free path can be associated with particle spacing or the grain size respectively.

The single parameter approach is inadequate to describe creep behaviour with primary, secondary and tertiary characteristics. Depending on the rate constants, it would be capable of describing either primary or tertiary creep under constant stress conditions but not on the same curve. It is related to an overall dislocation density and provides a very satisfactory description of monotonic deformation over large strain. However, fails to account for short transients associated with the beginning of plastic flow



or with jump wise changes in the deformation conditions. The main reason is the neglect of further static parameters whose fast relaxation may be responsible for transient behaviour. The resultant materials parameter  $\dot{\sigma}_s$  is temperature and strain rate dependent and  $n$  is temperature dependent at low temperature and constant at high temperature and  $\dot{\sigma}_s$  attains the Arrhenius type temperature dependence  $(\exp(-\frac{Q}{kT}))$  with  $Q$  being the activation energy for self diffusion.

The inadequacy of the single parameter approach is overcome by the introduction of another structure parameter, namely, the mobile dislocation density. It is natural choice because it is commonly viewed as a fast variable with respect to the forest dislocation density.

The sets of equations developed are general and flexible enough to be considered representative of most experimental situations. A framework for analysis is developed rather than a detailed investigation of specific situation. No term indicates that the behaviour of the considered cross section can be influenced by that of neighbouring ones.

### *Two Parameter Approach*

A one parameter model is usually sufficient for describing monotonic deformation, without abrupt changes of the deformation rate or the deformation path. To account for transients associated with such changes, a second 'rapid response' parameter is needed. A two parameter formulation was devised for this purpose. It distinguishes between the mobile dislocation density  $\rho_m$  and the density  $\rho_f$  of less mobile (forest) dislocations. Both are treated as internal variables obeying coupled evolution equations whose various terms account for major dislocation reactions involved. The one parameter variant of the model is obtained as a special case of the two parameter variable one. The need

for a second internal variable also arises when a complex strain hardening behaviour at large strains is to be accounted for.

Estrin and Kubin<sup>44</sup> considered mobile dislocation density  $\rho_m$  and the relatively immobile forest dislocation density  $\rho_r$  as two structural parameters that influence flow. They considered that these two quantities are coupled in their evolutionary behaviour as a result of the continuous immobilization of mobile dislocations during the process of straining and that, as the strain increases, they usually tend to saturate owing to a balance between production and concurrent recovery or annihilation events. The evolution equations for  $\rho_m$  and  $\rho_r$  as given by Estrin and Kubin<sup>44</sup> are:

$$\frac{1}{\rho_m b v} \frac{d\rho_m}{dt} = \frac{d\rho_m}{d\varepsilon} = \frac{C_1}{b^2} \left( \frac{\rho_r}{\rho_m} \right) - C_2 \rho_m - \frac{C_3}{b} \rho_r^{1/2} \quad 2.45a$$

$$\frac{1}{\rho_m b v} \frac{d\rho_r}{dt} = \frac{d\rho_r}{d\varepsilon} = C_2 \rho_m + \frac{C_3}{b} \rho_r^{1/2} - C_4 \rho_r \quad 2.45b$$

where  $C_1$  and  $C_2$  are numerical constants while  $C_3$ , and notably  $C_4$ , are generally strain rate and temperature dependent.

A constitutive model of plastic deformation has been proposed, based on two parameters related to the dislocation density. The model based on two structure parameters related to the dislocation density predicts the existence of negative branch of the strain-hardening rate at small plastic strains. The first term on the right hand side of equation (2.45) is a production term, with forest obstacles acting as pinning points for fixed dislocation source. The second term takes account of the mobile density decrease by interaction between mobile dislocations. The last term describes immobilization of mobile dislocation with a mean stress proportional to  $\rho_f^{-1/2}$ .

Generally, there is good accord between experiment and model prediction, which however becomes less satisfactory at large elongation, where a number of effects are not accounted for. The temperature dependence of parameters  $m$ ,  $n$  and  $\dot{\epsilon}_0$  is explicit and can be determined in standard experiments such as constant strain rate testing.

Some of the advantages of this approach are; a simple architecture of the equations with a relatively small number of parameters are involved, a simple relation of parameter to the microscopic properties or processes, a clear recipe for parameters evaluation, which, in combination with an evaluation strategy, can substantially simplify parameter identification and the model permits usage of its different variants.

Common features of this model to the one developed in this study are that in each case softening is a result of dislocation annihilation and the average/overall dislocation density is the principal feature of the material parameter with essentially the same fundamental kinetic relationship.

Unlike the Estrin – Mecking<sup>10</sup> approach, the present study is capable of describing secondary and tertiary creep on the same curve under constant creep and tensile loads conditions with the material parameter  $\dot{\epsilon}_s$  assumed constant with  $n$  being proportional to activation volume, stress and temperature and  $\dot{\epsilon}_0$  assumed constant.

Data from present study could not be used in Kocks-Mecking<sup>16</sup> model mainly because it is generally expected that the kinetic equation may be governed by more than one structure parameters evolving with different rates<sup>20</sup>. Each rate assuming a stationary value after a certain transient strain. Certainly, the latter depends on the current values of all the 'slower' structure parameters (still varying towards their saturation). Therefore, as deformation proceeds, more and more structure parameters will reach their saturation values so that eventually, at sufficiently large strains, only the slowest 'relaxation mode' associated with structure

parameter with the largest transient strain will survive. Others can be considered as instantaneous adapting to the current value of the slowest in the hierarchy of the structure parameters by assuming their stationary values which depend on the current value of the slowest one as well as on  $\dot{\epsilon}$  and  $T$ . It is this slowest varying structure parameter that is chosen in the one parameter approach with the average dislocation density chosen as the governing parameter.

## 2.6.2 Damage Mechanics

Damage of materials is caused by progressive changes in the internal structure of materials as an irreversible thermodynamical process. The predictive capabilities of the damage model depend strongly on its particular choice of damage variable. The selection of the damage variable is one of the most contentious aspects of damage mechanics. It is widely recognized that damage in metals is generally anisotropic, even if the material is initially isotropic<sup>47</sup>.

### *Creep – Damage Constitutive Equation*

Assuming creep potential as a function of the stress state and a set of internal variables, the following creep law can be formulated:<sup>48</sup>-

$$\dot{\epsilon} = \frac{\partial \Phi(\sigma_{eq}, H_i, \omega_k)}{\partial \sigma} \quad 2.46$$

$H_i$  and  $\omega_k$  denote two sets of hardening and damaging variables, respectively. This generalized creep damage law allows the reflecting of different damage and hardening processes. It can also be used for the primary creep.

In addition to the associated creep law, an evolution equation exists for the hardening and the damage variables<sup>48</sup>.

$$H_i = H_i(\sigma_{eq}^H, H_p, \omega_q, \dots) \quad 2.47$$

$$\omega_k = \omega_k(\sigma_{eq}^w, H_p, \omega_q, \dots) \quad 2.48$$

There are now three equivalent stresses which are in general different and are able to reflect various deformation mechanism influenced by different parts of the material .

The notion of damage in a phenomenological context is only very vague. It can be introduced into a mathematical model of the creep process in one of two ways. First, we can use the concept of a net stress,  $\sigma^*$ , such that if  $\sigma$  is the applied stress in a tensile test and  $\omega$  the damage (related to the reduction in area), then

$$\sigma^* = \frac{\sigma}{1 - \omega} \quad 2.49$$

Then, in order to describe the tertiary stage of the basic creep curve, the net stress is introduced into the constitutive equations developed for the primary and secondary stages. Alternatively, the damage may be introduced as a macroscopic internal variable. Suppose that, in the secondary phase of creep, the creep strain rate, which is constant, has the following functional dependence on stress

$$\dot{\epsilon}_c = f(\sigma) \quad 2.50$$

In order to account for the increase in strain rate in the tertiary phase, a new internal variable,  $\omega$ , is introduced in a way that as the damage increases the strain rate also increases.

$$\dot{\epsilon}_c = f(\sigma, \omega) \quad 2.51$$

The functional dependence of the strain rate on damage is assessed from the form of the basic creep curves assuming an initial value of damage as zero and a final value at rupture of unity. In either of these approaches, an equation relating the growth of damage to applied stress is required. This can take the form:-

$$\dot{\epsilon} = g(\sigma, \omega) \quad 2.52$$

and can generally be determined from the rupture curves.

For the damage evolution law an expression similar to the Norton law can be formulated<sup>12</sup>.

$$\dot{\epsilon}_c = B \frac{\sigma^{n_1}}{(1-\omega)^{n_2}} \quad 2.53$$

2.54

$$\omega = D \frac{\sigma^{k_1}}{(1-\omega)^{k_2}}$$

where  $B, D, n_1, n_2, k_1, k_2$  are material constants determined from the basic creep curves. If the concept of net stress is used, then  $n_1 = n_2 = n$  and  $k_1 = k_2 = k$ . The main Rabonov creep–damage equations enable an extension of the classical creep equation for stationary to the tertiary creep. The main problems are connected with the neglect of primary creep and the formal introduction of the damage parameter  $\omega$  that leads to a range of this parameter from zero (undamaged state) to one (fully damaged state) and which seems to be unrealistic. In addition, the damage law does not reflect the different damage behaviour, for instance, that resulting from tensile or compressive loads.

The two fundamental requirements for a set of creep damage constitutive equations to be developed are creep strain rate consistency and damage evolution consistency<sup>48</sup>.

One possible variation of the Rabotnov creep damage equation is given by the introduction of other expressions for the equivalent stress  $\sigma_{eq}^{\omega}$ . A suitable generalized equivalent stress expression was proposed, for instance, by Altanbach et al<sup>49</sup>. Starting from Novozhilov's stress tensor, invariants<sup>50</sup> the equivalent stress can be presented as follows:-

$$\sigma_{eq} = \lambda_1 \sigma_{vM} \sin \xi + \lambda_2 \sigma_{vM} \cos \xi + \lambda_3 \sigma_{vM} + \lambda_4 I_1 + \lambda_5 I_1 \sin \xi + \lambda_6 I_1 \cos \xi$$

$$\sin 3\xi = -\frac{27 \det s}{2\sigma_{vM}^3} \quad 2.56$$

For practical purpose mostly the proposal of Sdobyrev<sup>51</sup> and Leckie-Hayhurst<sup>52</sup> are mostly in use.

Recently, another set of creep damage equations has become popular. The starting point was the necessity to describe primary, secondary and tertiary creep for metallic materials. The following set of creep constitutive and evolution equations for different internal variables are recommended for ferritic steels.

The uni-axial form of creep damage constitutive equations for 0.5Cr-.5Mo-0.25V ferritic steel at 590°C are written as<sup>52</sup>.

$$\dot{\omega} = A \sinh \left( \frac{B\omega(1-H)}{(1-\Phi)(1-\omega)} \right) \quad 2.57$$

$$\dot{H} = \frac{h}{\sigma} \left( 1 - \frac{H}{H^*} \right) \dot{\omega}$$

$$\dot{\Phi} = \frac{k_c}{3} (1-\Phi)^4$$

$$\dot{\omega} = C \dot{\omega}$$

where  $A$ ,  $B$ ,  $C$ ,  $h$ ,  $H^*$  and  $K_c$  are material constants,  $H$  represents the strain hardening that occurs during primary creep; initially  $H$  is zero and as strain is accumulated, increases to the value of  $H^*$ .  $\Phi$  describes the evolution

of the spacing of the carbide precipitates, which are known to lead a progressive loss in the creep resistance of the particle hardened alloys as ferritic steels.  $\omega$  represents inter granular cavitations and varies from zero for material in virgin state to 1/3, when all the grain boundaries normal to the applied stress have completely caviatated.

The main problems associated with damage mechanics are:-

- Neglecting of the primary creep.
- The formal introduction of the damage mechanics parameter  $\omega$  that leads to a range of this parameter from zero (undamaged state) to one (fully damage state) and which seems to be not to be realistic.
- In addition, the damage law does not reflect the different damage behaviour, for instance, results from tensile or compressive loads.

### 2.6.3 The $\theta$ - Projection Techniques

The  $\theta$ -projection techniques are a procedure for interpolation and extrapolation of creep properties, some of which may have been obtained from accelerated tests. It is also useful as the basis for a constitutional relationship for component analysis for conditions of high temperature service. The variation in creep strain with time is outlined by the equation<sup>7</sup>:

$$\varepsilon = \varepsilon_o + \theta_1 [1 - \exp(-\theta_2 t)] + \theta_3 [\exp(\theta_4 t) - 1] \quad 2.58$$

where  $\theta_i$  (  $i=1,2,3,4$ ) designates constants which are determined by fitting the equation to the creep curves.

The first term in the equation (1) represents normal primary creep, while the second term describes tertiary behaviour. The minimum creep rate then emerges at the point of inflection. The fact that any creep curve can



be considered as the sum of decelerating primary and an accelerating tertiary component is the essential feature of the  $\theta$ - projection<sup>7</sup>.

$\theta_1$  = scales the primary strain.

$\theta_2$  = is a rate parameter governing the curvature of the primary stage.

$\theta_3$  = scales the tertiary strain.

$\theta_4$  = is a rate parameter governing the curvature of the tertiary stage.

$\theta$ -parameter varies systematically with stress and temperature, representing the changes in creep curve shape with changing test conditions, thus each value of  $\theta$  is a function of both temperature and stress.

$$\log \theta_i = a_i + b_i T + c_i \sigma + d_i \sigma T \quad 2.59a$$

$$\theta_i = a + bT + c\sigma + d\sigma T \quad 2.59b$$

The equation (2.59) was chosen on the basis of experimental creep data that reveals  $\ln \theta$  varied linearly with either temperature or stress<sup>52</sup>.

Evans et al<sup>53</sup> showed that at constant stress, creep tests carried out on 0.5Cr-0.5Mo-0.25V, a linear relationship characteristic of each creep temperature was obtained between stress and  $\ln \theta_i$  ( where  $i=1,2,3,4$ ).  $\theta$ -projection methods, however, considerably underestimate rupture lives for some other steels.<sup>54</sup> The variation of  $\theta$  parameters can be written as.

$$\left. \begin{aligned} \theta_1 &= G_1 \exp H_1 \left( \sigma / \sigma_y \right) \\ \theta_2 &= G_2 \exp - \left[ (Q_2 - H_2 \sigma) / RT \right] \\ \theta_3 &= G_3 \exp H_3 \left( \sigma / \sigma_y \right) \\ \theta_4 &= G_4 \exp - \left[ (Q_4 - H_4 \sigma) / RT \right] \end{aligned} \right\} \quad 5.60$$

G and H are material constants

$\theta_2$  = activation energy for self diffusion

$\theta_4$  = is the overall energy of several processes taking place at the tertiary stage. It is strongly influenced by mechanical instability and does not reflect the inherent material properties.

$\theta$  - projection technique gives a good representation of creep curves for moderate and high ductility engineering materials, but gives a poorer fit at low strains and times with difficulties in the prediction of low strains for low ductility materials.<sup>55</sup> Furthermore, the technique fails to account for changing strain due to localized neck formation, since method considers only uniform strain, ignoring the existence of a multi-axial stress state in that region<sup>56</sup>.

In the  $\theta$  - Projection technique, variations in  $n$  value are assumed to be not a consequence of change of dominant creep mechanism: Clearly, if different mechanisms controlled the creep properties exhibited within different stress/temperature regimes, analysing data collected in one mechanism regime could not predict the behaviour patterns in a different regime. The fact that extrapolation is accurate then supports the view that the same dislocation process is dominant. Furthermore, all  $\theta$ - projections are based on constant stress creep test data and not on constant load creep tests.

#### **2.6.4 Internal (Friction) Stress Method**

There is a considerable body of literature concerning the role of the possible internal stress ( $\sigma_i$ ) term but as yet there appears to be no satisfactory way of determining quantitatively how such a stress may vary during deformation. Furthermore, there is still much debate on physical interpretation of internal stress measurement. In glide-recovery models<sup>57-61</sup>, dislocation movement is considered to be opposed by an

'internal' or 'dislocation back stress',  $\sigma_i$ . The magnitude of the internal stress depends not only on the dislocation density but also on the heterogeneity of the dislocation substructure<sup>62-64</sup> and hence on a balance between strain hardening and recovery. The internal stress could be described as a measurement of the creep resistance of the microstructure with its magnitude depending on a number of parameters, such as applied temperature<sup>71</sup>, stress<sup>72</sup>, and the presence of second phase particles.

If the concept of friction stress is adopted, creep deformation is considered to take place not under the full applied stress but under an effective stress. The 'effective stress'  $\sigma_e$ , controlling the glide behavior of dislocations during creep under an applied stress,  $\sigma$ , is then given as<sup>7</sup>

$$\sigma_e = \sigma - \sigma_i \quad 2.61$$

with the internal stress being the driving force for recovery. Since the parameters characterizing the dislocation configurations established during creep change with stress,  $\sigma = \alpha Gb\sqrt{\rho}$  and  $\lambda = KGb/\sigma$ , a systematic dependence of the internal stress value on stress would be expected for measurements made during secondary creep. The data reported for a wide range of pure metals and single phase alloys has been collated.<sup>63</sup> A definitive relationship between internal stress and the applied stress does not always emerge, possibly because the behavior patterns displayed may vary depending on the material examined and on the precise stress-temperature conditions selected for investigation. The ratio  $\frac{\sigma_i}{\sigma}$  may be constant or may increase with decreasing stress for pure metals or class II alloys. While this type of behavior can also be true for class I alloys tested at low stresses,  $\sigma_i$  appears to be independent of stress when measurements are made for these types of alloys at high stresses<sup>7</sup>. For both iron and nickel alloys<sup>64</sup>

$$(\sigma - \sigma_0) \propto \sqrt{\rho} \quad 2.62$$

where  $\sigma_0$  was referred to as the 'internal or friction stress' introduced by the presence of alloying elements in the solid solution<sup>11</sup> or in the form of the precipitate<sup>63-64</sup>. Replacing the applied stress,  $\sigma$ , by the stress function  $(\sigma - \sigma_0)$  will generally result in an increased value for  $n$ .

The concept of internal stress pioneered by Wilshire and co-workers<sup>65-67</sup> has proved to be particularly useful in rationalizing the minimum creep rate data of engineering alloys, with the idea of recovery creep through the modified Bailey-Norton equation.

Using this concept, the creep data for single phase and multiphase alloys can be fitted to a modified form of Bailey – Norton equation.<sup>65-69</sup>

$$\dot{\epsilon}_s = k^* (\sigma - \sigma_0)^n \exp\left(-\frac{Q_c^*}{RT}\right) \quad 2.63$$

Where  $Q_c^*$  approximates that for lattice self diffusion and is measured from the temperature dependence of the secondary creep rate at constant  $(\sigma - \sigma_0)$  rather than at constant  $\sigma$ . Using values of  $\sigma_0$  determined by analysis of transient creep following stress reductions, the equation (2.63) yields values of  $n=4$  and  $Q_c^* \approx$  activation energy for self diffusion for a wide range of materials<sup>70-71</sup>,  $n$  is the exponent for the effective stress. However, the magnitude of  $\sigma_0$  is not constant for a particular alloy but has been reported to change with temperature<sup>72</sup> and stress<sup>73</sup> and to vary throughout creep life<sup>75-76</sup>.

In pure metals  $\sigma_0$  might arise from subcells or tangles, while in precipitation hardened systems a major factor will be the precipitation itself. With the introduction of  $\sigma_0$  the exponent  $p$  in

$\dot{\epsilon} = A(\sigma - \sigma_0)^p \exp\left(-\frac{\Delta G}{RT}\right)$  is now found to be  $\approx 4$  irrespective of

whether the data are for simple or complex materials. Furthermore, this approach results in a reduction of the anomalously high creep activation energies obtained on complex alloys, so that for all materials so far evaluated  $Q^*c$  can be related to appropriate activation energies for diffusion. On this basis it has been suggested that creep controlling mechanisms are similar<sup>65,67,72</sup> irrespective of the degree of material complexity.

Several investigators have used the internal stress approach in the study of low alloy ferritic steels. The section below highlights the merits and demerits of some of these investigations.

#### 2.6.4.1 Sidney's Approach<sup>3</sup>

Sidney's approach is based on Wilshire et al's<sup>65-67</sup> concept of friction stress. Creep tests at 823 and 838K in the stress range 220-340Mpa were carried out on a low alloy ferritic steel. Creep was resolved in terms of a recovery controlled model, using the concept of friction stress. Here, the steady state creep rate is related to the applied stress,  $\sigma_a$  and temperature by

$$\dot{\epsilon} = A(\sigma_a)^{17} \exp\left(-\frac{240000}{RT}\right) \quad 2.64$$

when creep measurements were considered in terms of  $(\sigma_a - \sigma_0)$  it was found that.

$$\dot{\epsilon} = A(\sigma_a - \sigma_0) \exp\left(-\frac{240000}{RT}\right) \quad 2.65$$

where  $A$  is a material constant, and  $R$  universal gas constant. Determination of the recovery behavior of the material was made by observing the strain time behavior upon reducing the initial applied stress by 5 percent during steady state creep. These tests were performed at a various initial applied stress levels between 225 and 340 MN/m<sup>2</sup> at both temperatures. In every case, following the instantaneous contraction of the

specimen, an incubation period of zero creep rates was observed before further creep tests took place at the reduced stress level. This indicated that recovery of the dislocation structure was taking place during the incubation period until the flow stress had been reduced sufficiently to allow further creep deformation to take place. These results show that under these particular tests conditions, the creep behavior of this alloy is recovery controlled. The friction stress measurements were made by reducing the applied stress during steady state creep by a small amount ( $-0.05\sigma_a$ ) and measuring the incubation period of zero creep rate.

The recovery rate was also considered in terms of  $(\sigma_a - \sigma_0)$  and was shown to be  $r\alpha(\sigma_a - \sigma_0)^4$ . Sidney also indicated that the steady state creep rate and recovery have similar stress dependences. The stress and temperature dependence of the creep rate were similar to those predicted by the recovery theory of creep. It was also observed that the fractional life spent in each of the three stages of creep was constant, irrespective of the stress or temperature. The tertiary stage occupied over 60 percent of the lifetime. These observations seem to be the common feature of low alloy steels<sup>80</sup>. It has been noted that such behavior holds irrespective of whether failure is by transgranular ductile or by intergranular brittle mode.

#### 2.6.4.2 Miller et al Approach<sup>82</sup>

Creep tests conducted between 823 K and 838 K in the stress range 90-365Mpa were carried out on a tempered bainitic structure. Creep was concluded to be recovery controlled and similar to that in Sidney's experiment<sup>3</sup>; friction stress measurements were used to reach this conclusion. The creep deformation of 1Cr-Mo-V in the tempered bainite condition at 838 and 823K can be represented by<sup>97</sup>

$$\dot{\epsilon} = \frac{AD_v Gb}{kT} \left( \frac{\sigma_a - \sigma_0}{G} \right)^{3.5} \quad 2.66$$

A graph of  $\log\left(\frac{\sigma - \sigma_o}{G}\right)$  against  $\frac{\dot{\epsilon}_s}{D}$  was plotted. David Millier<sup>82</sup> observed that there is a good agreement between the sets of data at 838 and 823 K. At each temperature, two regions are observed: at high stress (230Mpa) the strain rate has a stress exponent of 14 and at stresses below this the stress exponent is 4. Therefore, at higher stresses  $\propto \sigma^{14}$  and at low stress  $\propto \sigma^4$ , such behavior is typical of precipitation hardened alloys. This observed change in stress exponent is sometimes explained in terms of a change in mechanism, i.e., to behavior controlled by viscous drag or grain boundary sliding. However, the concept of friction stress is frequently used to explain the above change in stress exponent

The creep data for nimonic 90, MARM246 and H 46 steel correlate closely. However, the data for nimonic 75 and  $\alpha$ -iron are widely displaced from those of the complex alloys. In fact the ratio of maximum to minimum  $\left(\frac{\sigma - \sigma_o}{G}\right)$  is  $\approx 22$  at constant  $\frac{\dot{\epsilon}_s}{D}$  which is slightly inferior to the original  $(\sigma - \sigma_o)$  ratio of 16 at constant  $\dot{\epsilon}_s$ . The approximate superposition of the complex alloy data suggest that this approach gives some way towards describing creep behavior but deviations for simple phase materials indicate that all relevant factors are not taken into considerations. It is interesting to note that for nimonic 90 the stacking fault energy is relatively low, while for nimonic 75 and  $\alpha$ -iron it is high.

#### 2.6.4.4 Evans et al Approach<sup>73</sup>

Evans et al noted that a universal secondary creep rate for simple and complex materials based on equation  $\dot{\epsilon} = A \sigma^n \exp\left(-\frac{\Delta G}{RT}\right)$  is not possible. The discrepancies suggest that this equation does not provide an adequate description of creep behavior especially for low alloy steels.

According to Evans et al<sup>73</sup> creep, data for various alloys using friction stress can be calculated using a single universal equation. This involves

the normalization of the effective stress by the proof or yield stress of the alloy at the appropriate creep temperature. Since the flow stress of a material in tensile tests is also thought to be associated with the operation of dislocation sources, then it is possible that creep strength differentials may be related to tensile properties of the materials. The resultant expression been<sup>73</sup>:

$$\dot{\epsilon} = B \left( \frac{\sigma - \sigma_0}{\sigma_{0.05}} \right)^n \quad 2.67$$

where  $B$  is independent of the material, crystal lattice and microstructure and temperature.  $\sigma_{0.05}$  is the (high strain rate) yield stress and  $n = 3.5$  is confirmed on a variety of iron base alloys encompassing a variety of microstructure.

Generally, creep data for all the materials superimpose when the effective stress ( $\sigma - \sigma_0$ ) is nominated by the proof or yield stress and expressed as

$\log \left( \frac{\sigma - \sigma_0}{\sigma_{0.05}} \right)$  against  $\log \dot{\epsilon}$ . On this basis the ratio of maximum to minimum

$\left( \frac{\sigma - \sigma_0}{\sigma_{0.05}} \right)$  is 1.3 at constant  $\dot{\epsilon}$ . A considerable improvement on the value

of 22 for maximum to minimum ratio of  $\left( \frac{\sigma - \sigma_0}{G} \right)$ .  $\sigma_0$  tended to be large

for some material ( e.g. MARM 246) and small for some (e.g.  $\alpha$ -iron).

Little should be read into the relative magnitude of  $\sigma_0$  since, in any

material, it is dependent on temperature. For the creep temperature used

in Nimonic 75 and alloyed  $\text{Ni}_3\text{Al}$ ,  $\sigma_0$  increases with stress but  $\alpha$ -iron and

MAR-M246 it is stress –independent. With Nimonic 90 and H46 steel,  $\sigma_0$

is linearly dependent on stress at low stress but becomes stress-independent above 200 and 250MN/m<sup>2</sup> respectively.

Evans et al approach appears to be an improvement on Miller's approach mainly because of the improved correlation of data.



As stated previously, the creep properties of low alloy ferritic steels are very dependent on heat treatment and heterogeneity. Baird et al<sup>78</sup> studied the behavior of 1 percent Mo and 2 ¼ pct Cr-1 pct Mo ferritic steels in various microstructural forms and found that the creep was recovery controlled only under certain conditions of composition, initial structure and testing conditions. Thus recovery control was related to the presence of Mo<sub>2</sub>C and Mo<sub>2</sub>N particles in the matrix, whilst a solid solution mechanism was suggested as being important for non recovery controlled creep.

Myers et al<sup>79</sup> in a study of 1 percent CrMoV steel suggested that, although the creep strength varied with transformation product, their results could be rationalized using a solute drag model<sup>80</sup>. In this model it was assumed that the dislocations were pinned by the vanadium atoms in solution. A similar idea was proposed by Argent et al<sup>81</sup>. Such a model was at a variance with test conducted on a bainitic material where the stress reduction tests indicate recovery controlled creep<sup>80</sup>. Myers et al<sup>79</sup> based their model on the experimental observations of a sinh law relationship between the steady creep rate and the applied stress for various martensitic, bainitic and pearlitic micro-structures. However, a close inspection of their results for bainitic structures indicates that the creep behavior at 823k is better represented by  $\dot{\epsilon} = \epsilon_0 \sigma^n$ , where  $n$  is 16 at high stresses, reducing to 3.5 at low stresses. The change in slope occurred at about 230Mn/m<sup>2</sup>.

From all indication, the magnitude of  $\sigma_0$  is not constant for a particular alloy but has been reported to change with temperature<sup>83</sup> as well as stress<sup>84</sup> and to vary throughout creep life<sup>68</sup>. Furthermore, by arguing that time dependent coarsening of the microstructure reduces  $\sigma_0$  and thus, by implication, increases creep rate, Stevens and Flewitt<sup>85</sup> and Williams and Cane<sup>95</sup> have provided a plausible explanation of the extensive tertiary creep regime in engineering alloys such as the one under review.

## 2.7 Summary

Four empirical approaches namely;  $\theta$  projection techniques, Estrin-Mecking, Damage Mechanics and Internal Stress Methods have been analysed and compared with the concept used in this study; each with its merit and demerits outlined.

$\theta$  - projection technique gives a good representation of creep curves for moderate and high ductility engineering materials, but gives a poorer fit at low strains of times giving difficulties in the prediction of low strains for low ductility materials<sup>56</sup>.

Furthermore, the technique fails to account for changing strain due to localised neck formation, since the method considers only uniform strain, ignoring the existence of a multi-axial stress state in that region<sup>56</sup>.

Data from the present study can not be used in  $\theta$ - projection, primarily because quantities measured are different and also because in this study a basic premise of the power law creep approach is that variations in  $n$ ,  $m$  and  $Q$  are a consequence of different mechanisms becoming dominant in different stress/temperature regimes. Furthermore, results are based on constant load creep test and tensile data.

In the  $\theta$  - Projection technique, variations in  $n$  value are assumed not to be a consequence of change of dominant creep mechanism: Clearly, if different mechanisms controlled the creep properties exhibited within different stress/temperature regimes, analysing data collected in one mechanism regime could not predict the behaviour patterns in a different regime. The fact that extrapolation is accurate then supports the view that the same dislocation process is dominant. Furthermore, all  $\theta$ - projections are based on constant stress creep test data and not on constant load creep tests.

The similarities of the concept with the one being proposed lies primarily in the fact that creep and recovery are by dislocation re-arrangement and annihilation processes.

### *Estrin –Mecking*

Unlike the Estrin – Mecking approach, the present study is capable of describing secondary and tertiary creep on the same curve under constant creep and tensile load conditions with the material parameter  $\sigma_s$  is assumed constant and  $n$  is proportional to activation volume, stress and temperature with  $\epsilon_{\&}$  assumed constant.

Generally, there is good accord between experiment and model prediction which however becomes less satisfactory at large elongation, where a number of effects are not accounted for. The temperature dependence of parameters  $m$ ,  $n$  and  $\&$  is explicit and can be determined in standard experiments such as constant strain rate testing. Kocks-Mecking approach is of restricted application, for it is generally expected that the kinetic equation may be governed by more than one structure parameter evolving with different rates<sup>20</sup>.

The sets of equations developed are general and flexible enough to be considered representative of most experimental situations. However, with this concept a framework for analysis is developed rather than a detailed investigation of a specific situation. No term indicates that the behaviour of the considered cross section can be influenced by that of neighbouring ones.

### *Creep Damage*

Creep damage mechanics are very complex, requiring more time and advanced techniques for their application, compared to the present study. The general constitutive equations require to be modified for the low alloy ferritic steel used in this study, even though in these materials

tertiary creep predominates. Creep mechanics models are based primarily on void growth, a mechanism different from the dislocation re-arrangement and annihilation used for this study.

As with the Hull –Rimmer model<sup>50</sup> which assumes that void growth is controlled by grain boundary diffusion, other void growth models have been proposed, for example, growth controlled by surface diffusion and growth by power law creep<sup>51</sup>. During the last stages of a creep test, it is unlikely that any of the above mechanisms are strictly true description of behaviour since final fracture is liable to be controlled by coalescence of voids or cracks and propagation of micro cracks. Data from the present study can not be used in the creep damage equation for ferritic steel since quantities measured are different from those used in creep damage mechanics.

### *Internal Stress*

Sections 2.6.4.1, 2.6.4.2 and 2.6.4.3 dealt with models that assume that deformation is a function, not simply of applied stress, but also of the applied stress minus an internal stress. If the internal stress were to increase as deformation proceeds, then a falling strain rate with increasing time or strain is obtained. The probability that a flow event occurs is expressed as an Arrhenius term involving the activation energy. A way in which primary creep may be described is to assume that this probability is a function of the applied stress and the internal structure or degree of hardening of the material, as well as the of the activation energy for the particular mechanism under consideration. The stress dependence of the apparent activation energy exists as well as the additional assumption that the apparent activation energy is also dependent on the degree of work-hardening<sup>88</sup>

To date  $\sigma_o$  measurements have been made only on a limited number of materials. From all measurements of friction stress reported it appears that they fall into two categories:- the stress drop technique during

creep tests and stress relaxation during a constant strain rate test. These techniques have been reviewed by Bolton<sup>87</sup>. However, there is still some controversy both in the methods of determining friction stress and in its physical interpretation.

The creep stress can be considered to comprise two components; an athermal internal stress and a thermally dependent effective stress, with the former providing the driving force for recovery and the latter that for dislocation glide. Controversy has arisen over the contribution of each to the total applied stress. In Sidney<sup>3</sup>, an incubation period of zero creep was always observed whenever a small stress reduction was made during steady-state creep, indicating that time was required for recovery of the dislocation network before further creep would proceed. Therefore, these results support the view that the internal stress is approximately equal to the applied stress for steady-state creep.

For precipitate hardened alloys it has been suggested that the internal stress consists of two components, namely, that due to the dislocation structure and that due to the dispersion of particles. The stress dependence of the steady creep—rate depends on the magnitude and stress dependence of the friction stress. The friction stress is large and decreases slightly as the applied stress increases. This gives rise to the high value of the stress exponent obtained when the steady creep-rate is considered in terms of the applied stress.

In concluding, therefore, the parameter of friction stress is a very useful concept in the understanding of the creep behaviour of a wide range of precipitate hardened alloys. It can be also be used to asses the influence of a change in microstructure due to long term ageing on the creep properties. This is very useful in micro structurally unstable alloys such as ferritic steels , in which in some cases damage is thought to occur through microstructural effect rather than the usual cavity formation. However, its practical use in life prediction has still to be proved experimentally, the main difficulties are the problems of measurement of friction stress at very low applied stress. In fact, it is almost impossible to

account for the friction stress at low stress because of the limited strain rate. A possible means of overcoming the problem of determination at low service stresses proposed by Cane and Williams<sup>86</sup> is very complicated.

The major obstacle with the concept is that extrapolation for long ageing time is unreliable because of the unstable nature of these alloys. The microstructure changes with ageing time causing decrease in creep resistance of the alloys, and the effective stress is difficult to obtain because of the uncertainty associated with measurement of the internal stress.

The data from present study can be used in the internal stress technique if some modification to the model is effected. Microanalyses revealed no coarsening, mainly because of the short duration of tests. Thus it would be safe to assume that internal stress change due to micro structural changes was not significant enough to justify its measurements which by all account are very difficult to perform particularly at low strain rate. Thus it would be safe to assume that changes in internal stress values will have been very slight, meaning that applied strength would have been only slightly higher than that the effective stress, particularly during the secondary creep stage.

### *Conclusion*

Discussions of the four methods clearly show that, with the exception of the internal stress concept the three other concepts do not adequately represent the concept being adopted in this study. The methods discussed here are of varying complexity. Both the  $\theta$  projection and damage mechanics approaches are by far the most complex when compared to either Estrin-Mecking and the internal stress concept and, for that matter the concept used in this study. Generally, to only a limited extent for the Estrin-Mecking concept, techniques used in the determination of materials parameters for the four concepts are very tedious and complex.

Investigation of creep mechanism of the low alloy steels using these approaches required modifications. In the case of damage mechanics, sets of constitutive equations were required to describe the creep curve. For these varied sets of parameters were calculated. This has been amply illustrated<sup>50</sup>.

In the  $\theta$  projection approach, Evans et al<sup>53</sup> had some success for low alloy steels, even though the method considerably underestimated rupture lives for some other steels.

The major advantages of the present concept compared to the  $\theta$  projection, damage mechanics and internal stress approaches are: that the test method used is simpler and are cost effective and that data manipulation is simpler and quicker, a simple architecture of the equations with a relatively small number of parameter involved, simple relation of parameter to the microscopic properties or processes and a clear recipes for parameters evaluation, which, in combination with an evaluation strategy, can substantially simplify parameter identification.